ISSN 2616-7433 Vol. 3, Issue 8: 1-7, DOI: 10.25236/FSST.2021.030801

A novel Model Predictive Current Control of Interior Permanent Magnet Synchronous Motor powered by Three-phase Four-switch Voltage-source Inverter

Ting Yang[1,2,a*], Yan Li[1,b], Liqing Ren[1,2,c], Min Guo[1,d], Xiong Wang[1,e]

[1]*School of Energy Engineering, Yulin University, Yulin, 719100, China;*
[2]*Laboratory of Coherent Raman Scattering, Yulin University, Yulin 719000, China*
[a]*yt871028@163.com,* [b]*yezi0117@163.com,* [c]*liqing_ren@yulinu.edu.cn,* [d]*281366282@qq.com,* [e]*12296832@qq.com*
[*]*Corresponding Author*

Abstract: *In this study, a novel model-predictive-current-control (MPCC) is developed and implemented based on an interior permanent magnet synchronous motor(IPMSM) drives fed by three-phase four-switch voltage-source inverter (TPFS-VSI) with fewer switches and lower costs. Compared with the conventional MPCC method, the complicated weighting factors designing process is avoided and it can greatly reduce the d-q axes currents and three-phase current ripples. Finally, MATLAB/Simulink simulation results validate the effectiveness of the proposed method .*

Keywords: *Model-predictive-current-control (MPCC),Interior permanent magnet synchronous motor (IPMSM), Three-phase Four-switch Voltage-source Inverter (TPFS-VSI)*

1. Introduction

IPMSMs have been widely used in many applications such as electric vehicles, air conditioning compressors and machine tool spindle drives due to their many advantages such as high efficiency, high power density, high torque-to-inertia ration, wide speed operation range and maintenance free operation [1,2]. TPFS-VSI as a topological structure of a three-phase six-switch voltage-source inverter (TPSS-VSI) is beneficial to improve the operational reliability of IPMSM,so it has been widely used in the drive system of IPMSMs. It is a cost effective solution replacing the (TPSS-VSI) because of the ease of its control structure and reduced complexity [3]. For IPMSM drive systems, MPCC is an emerging control strategy [4, 5], which adopts the principle of model predictive control (MPC). MPC strategies have the ability to deal with system constraints, multi-objective optimization and multi-variable control problems, and have been widely used in the control of power electronic converters.

In this paper, a novel model-predictive-current-control (MPCC) is developed and implemented based on an interior permanent magnet synchronous motor(IPMSM) drives fed by three-phase four-switch voltage-source inverter (TPFS-VSI). Compared with the conventional MPCC method, the complicated weighting factors designing process is avoided and it can greatly reduce the d-q axes currents and three-phase current ripples. The simulation results validate the effectiveness of proposed method.

2. IPMSMs drive system

2.1 Mathematical model of IPMSM

The IPMSM model in the rotor rotating(d-q) reference frame could be written as:

$$u_d = \mathrm{R_s} i_d + p\psi_d - \omega_e \psi_q \tag{1}$$

$$u_q = \mathrm{R_s} i_q + p\psi_q + \omega_e \psi_d \tag{2}$$

ISSN 2616-7433 Vol. 3, Issue 8: 1-7, DOI: 10.25236/FSST.2021.030801

$$\begin{aligned}\psi_d &= L_d i_d + \psi_f \\ \psi_q &= L_q i_q\end{aligned} \tag{3}$$

$$T_e = 1.5 P_n i_q \left(\psi_f + (L_d - L_q) i_d\right) \tag{4}$$

The voltage and flux torque equations of IPMSMs are given in (1)-(4), where u_d/u_q, i_d/i_q, L_d/L_q, Ψ_d/Ψ_q are the d-q axes voltages, currents, inductances and stator flux-linkages, respectively, R_s is the stator resistance, p is d/dt, ω_e is the electric angular velocity, and Ψ_f is the permanent magnet flux linkage.

2.2 Three-phase four-switch voltage-source inverter

The drive system on the basis of IPMSMs is shown in Figure 1 (a), where V_{dc} is the DC-link voltage, C_1 and C_2 are the upper and lower capacitors, S_j and S_{j1} (j=a,b,c) are the up and low switches which are composed of insulated gate bipolar transistors (IGBTs) and antiparallel diodes.K_a, K_b, and K_c are added between the middle point of the dc-link capacitors ('o' as defined in Figure 1(a)) and the output terminal of the VSI.

In normal operation mode, K_a, K_b, and K_c are all in off state and the three-phase stator voltages in *abc*-system are given by(5).

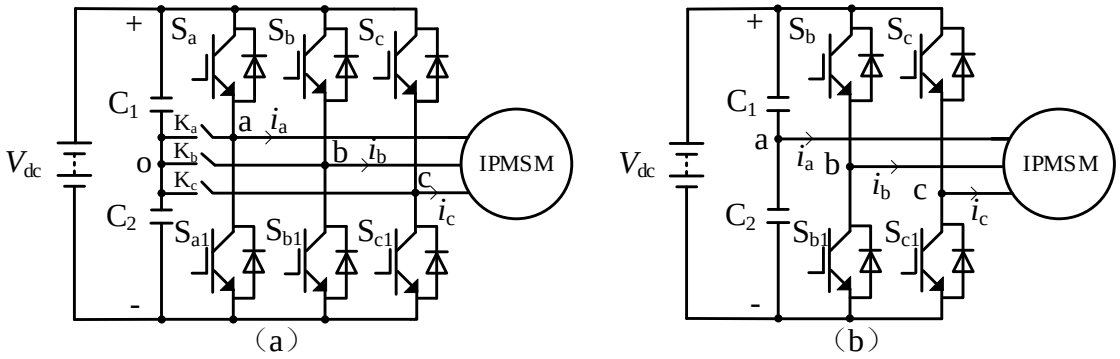

Figure 1. Drive system on the basis of IPMSMs (a)TPSS-VSI(b)TPFS-VSI

$$\begin{cases} U_a = \dfrac{U_{dc}}{3}(2S_a - S_b - S_c) \\ U_b = \dfrac{U_{dc}}{3}(2S_b - S_a - S_c) \\ U_c = \dfrac{U_{dc}}{3}(2S_c - S_a - S_b) \end{cases} \tag{5}$$

When one of the phases(for example phase a) has an open-circuit fault, the bidirectional thyristor of the corresponding phase is closed, and the output terminal of the fault phase is connected to the middle point of the dc-link capacitors to make the circuit show as Figure1(b), which is the so-called TPFS-VSI .

Figure 1 (b), the DC-link voltage is divided into two voltage source by capacitors C_1 and C_2,and the winding of phase a of the IPMSM is connected to the middle of two capacitors,so the terminal voltage of phase a is 0,while for phases b and c, the terminal voltage is equal to the voltage of C_1 (U_{c1}) with S_j switching on, and it is equal to the negative voltage of C_2 ($-U_{c2}$) with S_j switching off. The switching states are defined as '1' and '0' for the former and latter cases, respectively. Considering all the possible switching combinations of the gating signals S_b and S_c ,only four voltage vectors are consequently obtained which are shown in Figure 2(b) and listed in Table 1. The number of space vectors has been decreased from 7 to 4 by comparing with the TPSS-VSI in αβ-plane.

ISSN 2616-7433 Vol. 3, Issue 8: 1-7, DOI: 10.25236/FSST.2021.030801

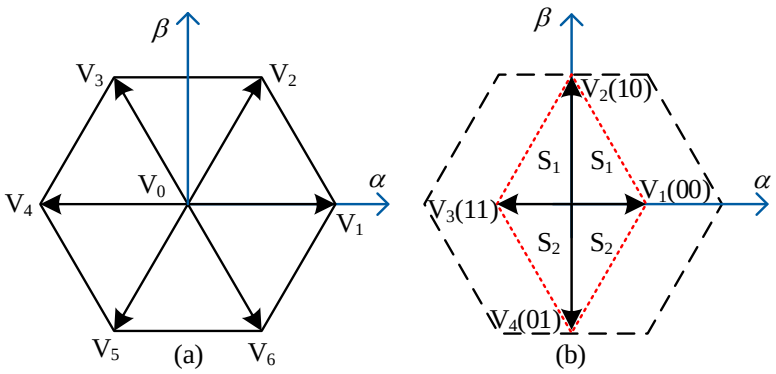

Figure 2. Space vector diagrams. (a) TPSS-VSI. (b) TPFS-VSI

Table 1 Switching states and voltage vectors of TPFS-VSI

S_b	S_c	Symbol V_i	Value
0	0	V_1	$2u_{c2}/3$
0	1	V_4	$(u_{c2}-u_{c1})/3 - j(u_{c1}+u_{c2})/\sqrt{3}$
1	0	V_2	$(u_{c2}-u_{c1})/3 + j(u_{c1}+u_{c2})/\sqrt{3}$
1	1	V_3	$-2u_{c1}/3$

The three-phase stator voltages in *abc*-system are given by(6).

$$\begin{cases} u_a = \frac{u_{c1}}{3}(-S_b - S_c) + \frac{u_{c2}}{3}(2 - S_b - S_c) \\ u_b = \frac{u_{c1}}{3}(2S_b - S_c) + \frac{u_{c2}}{3}(2S_b - S_c - 1) \\ u_c = \frac{u_{c1}}{3}(2S_c - S_b) + \frac{u_{c2}}{3}(2S_c - S_b - 1) \end{cases} \tag{6}$$

3. The proposed Model Predictive Current Control method

The current predictive equations can be obtained by discretizing (1) and (2) they are given in (3) and (4), where T_s is the sampling period and k is the number of T_s.

$$i_d(k+1) = (1 - R\frac{T_s}{L_d})i_d(k) + \omega_e T_s i_q(k)\frac{L_q}{L_d} + \frac{T_s}{L_d}u_d(k) \tag{7}$$

$$i_q(k+1) = (1 - R\frac{T_s}{L_q})i_q(k) - \omega_e T_s i_d(k)\frac{L_q}{L_d} + \frac{T_s}{L_q}u_q(k) - \omega_e T_s\frac{\psi_f}{L_q} \tag{8}$$

Because the midpoint of the dc-link capacitors is connected with phase a, the difference between the voltage of C_1 and C_2 (V_{c_e}) can be calculated by (9).

$$C\frac{d(V_{c1} - V_{c2})}{dt} = C\frac{dV_{c\_e}}{dt} = i_a \tag{9}$$

Where V_{c1}, V_{c2} are the voltage of C_1 and C_2, and i_a is the current of phase 'a'. Then, the predictive equation of V_{c_e} is given in (10).

$$V_{c\_e}(k+1) = V_{c\_e}(k) + i_a\frac{T_s}{C} \tag{10}$$

ISSN 2616-7433 Vol. 3, Issue 8: 1-7, DOI: 10.25236/FSST.2021.030801

According to the Table 1, the positions of V_1 and V_3 are always line in the α-β axis,but the positions of V_2 and V_4 will be changed when the V_{c1} is not equal to V_{c2} as shown in Figure. 4(b) and (c), the space vector diagram can be divided into 2 sectors, i.e., S_1 and S_2. Sector S_1 consists of V_1, V_2, and V_3. Sector S_2 consists of V_1, V_3, and V_4.

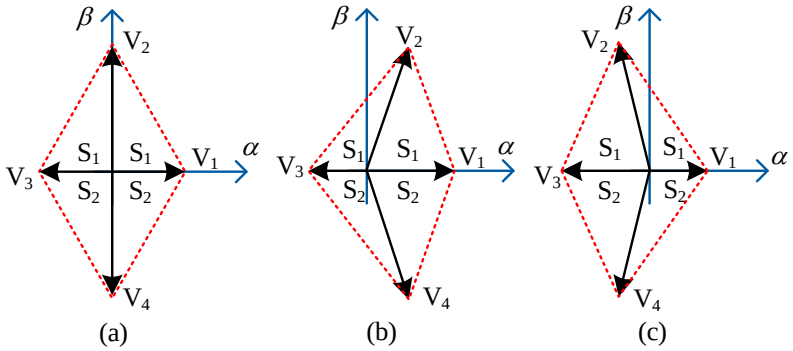

Figure. 4 Space vector diagram for TPFS-VSI. (a) $V_{c1}=V_{c2}$ (b) $V_{c1}<V_{c2}$ (c) $V_{c1}>V_{c2}$.

According to the nearest-three-vectors (NTVs) principle, when V_1, V_2, and V_3 are selected as the NTVs, and the pulse sequence is shown in Figure. 5(a). Otherwise, V_1, V_3, and V_4 are selected as the NTVs, and the pulse sequence is shown in Figure. 5 (b). The t_1-t_4 are the durations of V_1-V_4, t_b and t_c are the durations of state '1' of phase 'b' and 'c', respectively.

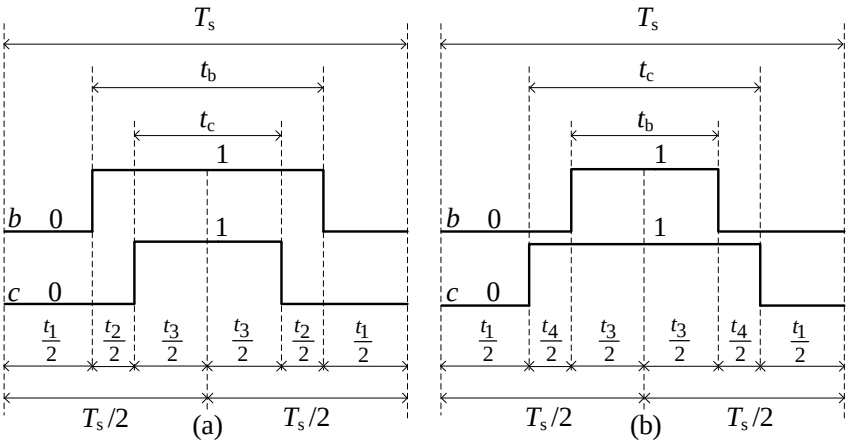

Figure. 5 Pulse sequence diagram (a) Sequence 1 (b) Sequence 2

The optimized pulse sequence can be selected according to (11) where an evaluation criteria g_1 is defined in (12). If S is 1, the sequence 1 is selected; Otherwise, the sequence 2 is selected.

$$S=\begin{cases}1, g_1(V_2)<g_1(V_4)\\ 2, g_1(V_2)>g_1(V_4)\end{cases} \tag{11}$$

$$g_1=(i_d^*-i_d(k+1))^2+(i_q^*-i_q(k+1))^2 \tag{12}$$

Where the i_d^*, i_q^* are the reference of d-q axis current , $i_d(k+1)$ and $i_q(k+1)$,are the current predictive .

Taking the pulse sequence 1 as an example, Figure. 6 shows the trajectory of with the pulse sequence 1.

ISSN 2616-7433 Vol. 3, Issue 8: 1-7, DOI: 10.25236/FSST.2021.030801

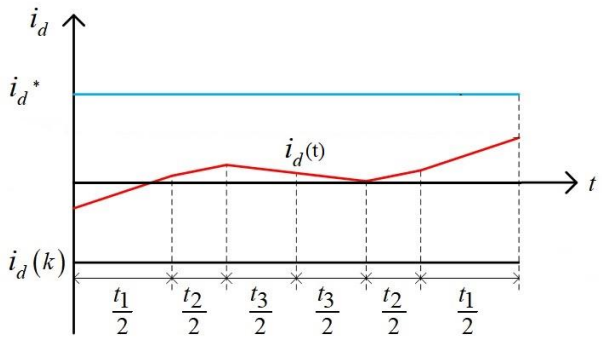

Figure. 6 Trajectory of with the pulse sequence 1

According to Figure. 6 ,(13) can be obtained.

$$\begin{cases} i_d^* = i_d(k) + k_{1d}(T_s - t_b) + k_{2d}(t_b - t_c) + k_{3d}t_c \\ i_q^* = i_q(k) + k_{1q}(T_s - t_b) + k_{2q}(t_b - t_c) + k_{3q}t_c \end{cases} \tag{13}$$

The results are given in (14) satisfy (15).

$$\begin{cases} t_b = (m_1 d_1 - b_1 n_1)/(a_1 d_1 - b_1 c_1) \\ t_c = (a_1 n_1 - c_1 m_1)/(a_1 d_1 - b_1 c_1) \end{cases} \tag{14}$$

$$\begin{cases} m_1 = i_d^* - i_d(k) - k_{1d}T_s \\ n_1 = i_q^* - i_q(k) - k_{1q}T_s \\ a_1 = k_{2d} - k_{1d},\ b_1 = k_{3d} - k_{2d} \\ c_1 = k_{2q} - k_{1q},\ d_1 = k_{3q} - k_{2q} \end{cases} \tag{15}$$

Where the $m_1 = i_d^* - i_d(k) - k_{1d}T_s$; $d_1 = k_{3q} - k_{2q}$; $b_1 = k_{3d} - k_{2d}$; $n_1 = i_q^* - i_q(k) - k_{1q}T_s$;

$a_1 = k_{2d} - k_{1d}$; $c_1 = k_{2q} - k_{1q}$.

The duty cycle of phase b and c can be caculated by (16)

$$\begin{cases} D_b = t_b/T_s \\ D_c = t_c/T_s \end{cases} \tag{16}$$

According to the inject a dc offset to i_a, so if changing t_1 and t_3 can be changing the durations of V_1 and V_3.

4. Simulation results

To validate the effectiveness of the proposed MPCC of IPMSMs system fed by TPFS-VSI, a simulation model has been established and the main parameters are given in Table 2.

Table 2 Parameters of the IPMSM

Parameter	Value
V_{dc}	540V
C_1,C_2	4.2mF
ψ_f	0.225Wb
L_d/L_q	0.95/2.1mH
R	0.1Ω
P_n	4
T_s	1e-4s

ISSN 2616-7433 Vol. 3, Issue 8: 1-7, DOI: 10.25236/FSST.2021.030801

The curves of d-q axes current for the conventional and proposed MPCC are shown in Figure. 7 and Figure. 8, respectively. In the middle of Figure. 7 and Figure. 8, the load torque changes from 50Nm to 100Nm.

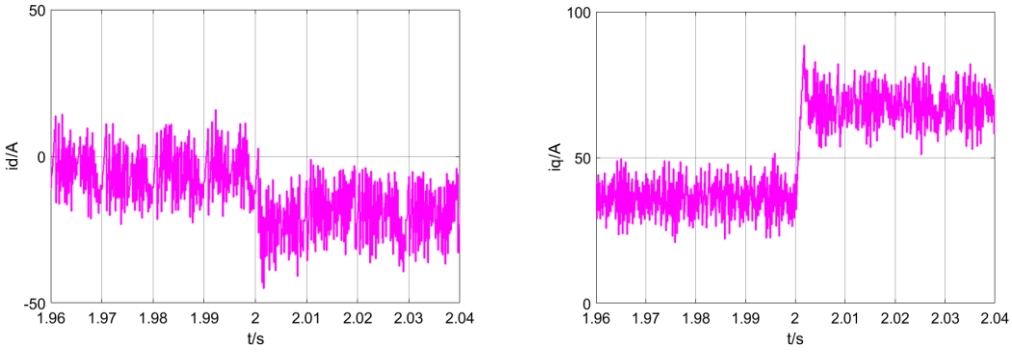

(a) *(b)*

Figure. 7 Curves of d-q axes current for the conventional method. (a) i_d. (b) i_q.

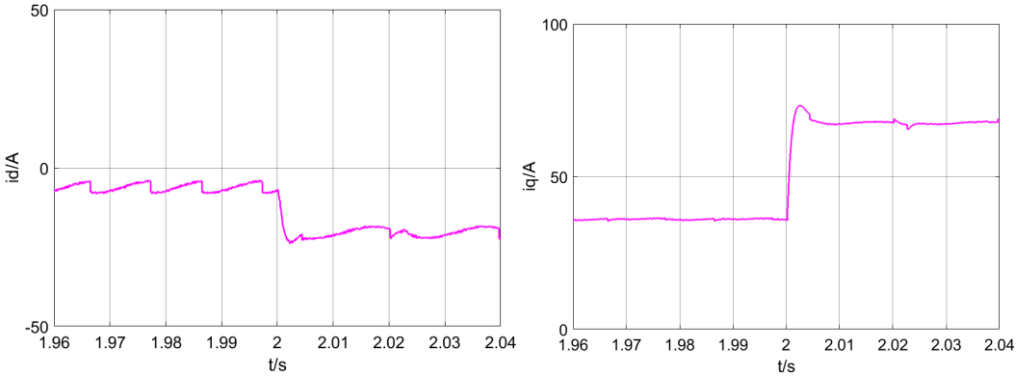

(a) *(b)*

Figure. 8 Curves of d-q axes current for the proposed method. (a) i_d. (b) i_q.

It can be seen from the Figures. 7 and 8, compared with the conventional method, the d-q axes current ripples can be greatly suppressed.

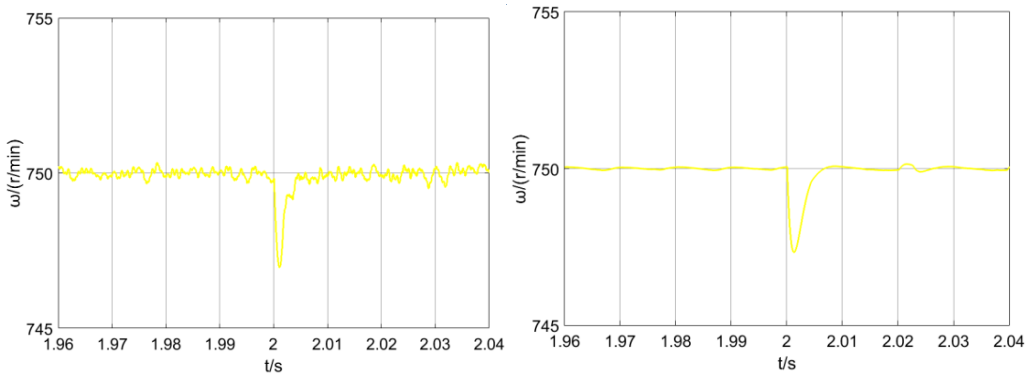

(a) *(b)*

Figure. 9 Curves of speed for the conventional and proposed MPCC.(a)Conventional. (b) Proposed .

5. Conclusion

A novel model-predictive-current-control (MPCC) of interior permanent magnet synchronous motor (IPMSM) drives fed by three-phase four-switch voltage-source inverter (TPFS-VSI) is studied. The proposed MPCC method selects an optimized sequence and the durations of space vectors is given to realize the tracking of i_d^* and i_q^*. The capacitor voltage balance method by injecting a dc offset to

ISSN 2616-7433 Vol. 3, Issue 8: 1-7, DOI: 10.25236/FSST.2021.030801

the current of fault phase is also given. The simulation results indicate the effectiveness of the proposed method and the d-q axes current ripples have been greatly decreased compared with the conventional method.

Acknowledgment

The project is partially supported by the National Natural Science Foundation of China under Grant12064046.The project is partially supported by Industry-academia research project of Yulin Science and Technology Bureau under award CXY-2020-008-02 and Yulin High-tech Zone 2020 Science and Technology Plan Project under award CXY-2020-38.

References

[1] M. Siami, D. A. Khaburi, M. Rivera, and J. Rodr ́guez (2017). An Experimental Evaluation of PredictiveCurrent Control and Predictive Torque Control for a PMSM Fed by a Matrix Converter[J]. IEEE Transactions on Industrial Electronics, vol. 64, no. 11, pp. 8459-8471.

[2] Hoang, K. D.; Zhu, Z. Q.; Foster, M. P (2011). Influence and Compensation of Inverter Voltage Drop in Direct Torque-Controlled Four-Switch Three-Phase PM Brushless AC Drives[J]. IEEE Trans. Power Electron. 26, 2343-2357.

[3] Z. Zhou, C. Xia, Y. Yan, Z. Wang, and T. Shi (2017). Torque Ripple Minimization of Predictive Torque Control for PMSM With Extended Control Set, IEEE Transactions on Industrial Electronics, vol. 64, no. 9, pp. 6930-6939.

[4] Kivanc O, Ozturk S(2019,). Low-Cost Position Sensorless Speed Control of PMSM Drive Using Four-Switch Inverter [J]. Energies, 12, 741.

[5] Q. F. Teng, J. Y. Bai, and J. G. Zhu (2013). Fault Tolerant Model Predictive Control of Three-Phase Permanent Magnet Synchronous Motors[J]. WSEAS Transactions on systems, 8(12):385-397 .